ACS PHYSICAL CHEMISTRY Au
AN OPEN ACCESS JOURNAL OF THE AMERICAN CHEMICAL SOCIETY

pubs.acs.org/physchemau
Letter

Optically Gated Dissociation of a Heptazinyl Radical Liberates H• through a Reactive $\pi\sigma^*$ State

Published as part of ACS Physical Chemistry Au virtual special issue "Ultrafast Spectroscopy of Chemical Transformations".

Liam Wrigley,[⊥] Doyk Hwang,[⊥] Sebastian V. Pios, and Cody W. Schlenker*

Cite This: *ACS Phys. Chem Au* 2024, 4, 598–604

ABSTRACT: Using trianisole heptazine (TAHz) as a monomeric analogue for carbon nitride, we performed ultrafast pump–photolysis–probe transient absorption (TA) spectroscopy on the intermediate TAHzH• heptazinyl radical produced from an excited state PCET reaction with 4-methoxyphenol (MeOPhOH). Our results demonstrate an optically gated photolysis that releases H• and regenerates ground state TAHz. The TAHzH• radical signature at 520 nm had a lifetime of 7.0 ps, and its photodissociation by the photolysis pulse is clearly demonstrated by the ground state bleach recovery of the closed-shell neutral TAHz. This behavior has been previously predicted as evidence of a dissociative $\pi\sigma^*$ state. For the first time, we experimentally demonstrate photolysis of the TAHzH• heptazinyl radical through a repulsive $\pi\sigma^*$ state. This is a critical feature of the proposed reaction mechanisms involving water oxidation and CO_2 reduction.

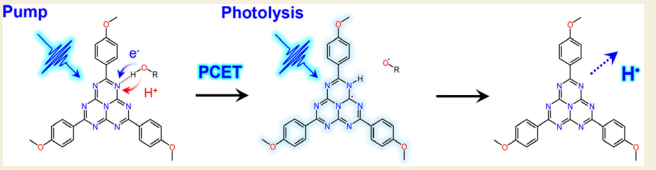

KEYWORDS: *Carbon nitride, Photoreduction, Photochemistry, Solar energy, Photocatalysis, Photoredox catalysis*

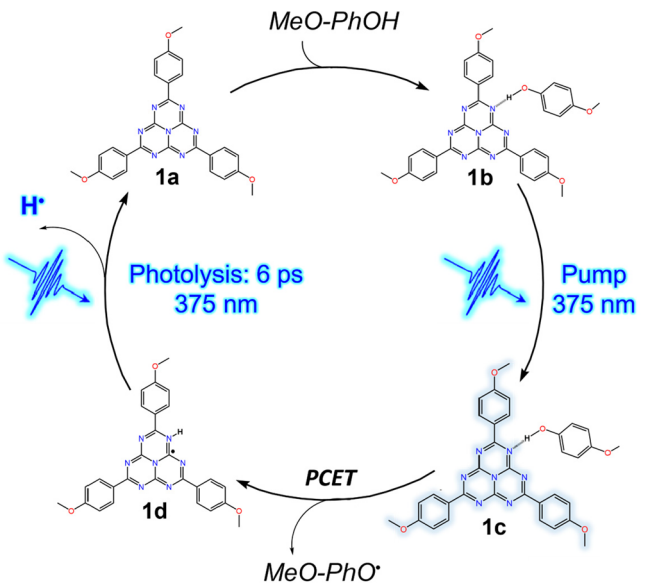

Figure 1. Optically gated reaction cycle performed in toluene. First, there is preassociation of methoxyphenol to TAHz **1a**. Then, a pump pulse of 375 nm excites the TAHz:MeOPhOH complex **1b** to **1c** followed by PCET forming the TAHzH• heptazinyl radical **1d**. A subsequent photolysis pulse at 6 ps leads to the photodissociation of the TAHzH• heptazinyl radical to release H• and regenerate the closed-shell ground state TAHz.

Proton-coupled electron transfer (PCET)[1,2] reactions are fundamental processes in many biological and chemical systems, such as photosynthesis,[3,4] respiration,[5,6] and catalysis.[7] Heptazines can undergo PCET processes with protic substrates, such as water or phenols, to form a highly reactive heptazinyl radical species (HzH•) that has been calculated to have a dissociation energy of 2.0 eV (46 kcal/mol).[8] Heptazines are monomeric units of carbon nitride[9−11] and can be considered a testbed for understanding carbon nitride photoreactivity.[12] While carbon nitride has been modeled by some as an organic semiconductor,[13] due to the disparity between the time scales of charge transfer dynamics and the photoreactivity observed[14−16] it has also been modeled as a localized molecular photocatalyst,[17−19] where intermediate steps include heptazinyl radicals.[20−22] For example, Merschjann et al. have performed detailed photoluminescence[23] and time-resolved photoelectron spectroscopy (TRPES)[24] studies that support an electronic treatment of 2-D carbon nitride as heptazine quasi-monomers at these time scales.[25]

In our studies of a functionalized monomer of carbon nitride, trianisole heptazine (TAHz), we have observed

Received: April 19, 2024
Revised: June 21, 2024
Accepted: June 25, 2024
Published: July 5, 2024

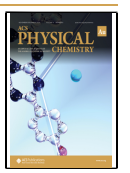

https://doi.org/10.1021/acsphyschemau.4c00030
ACS Phys. Chem Au 2024, 4, 598–604

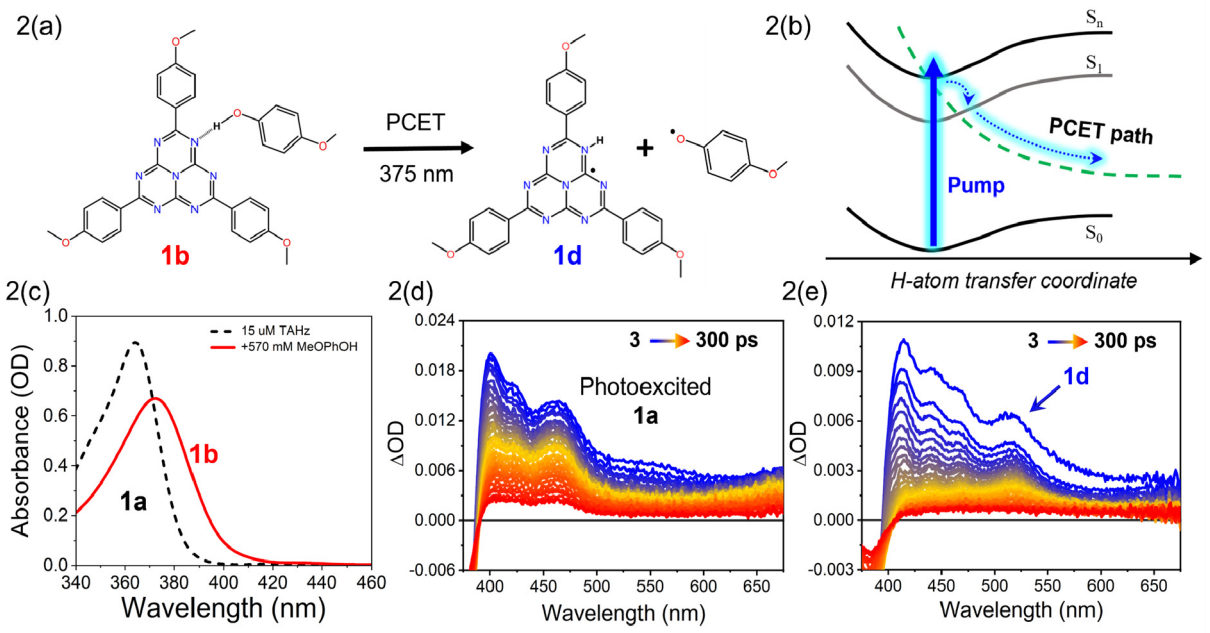

Figure 2. Summary of the PCET reaction step. (a) Reaction scheme for TAHz:MeOPhOH undergoes a PCET barrierless transition to the TAHzH$^{\bullet}$ radical. (b) Energy level diagram showing how the pump pulse (375 nm) excites to higher S_n energy levels that exhibit higher oscillator strength, and as it relaxes to S_1, a fraction of the excited state population branches off into a CT state. (c) Absorption spectrum for ground state TAHz **1a** and the TAHz:MeOPhOH complex **1b**, showing the redshift of the hydrogen bonded complex. (d) Summary of data from ref 46. Transient absorption of TAHz **1a** without PCET displays an excited state absorption signal related to the S_1 energy level. (e) Transient absorption spectrum of TAHz:MeOPhOH with a 375 nm pump displays a 520 nm signal associated with **1d**. Adapted with permission from ref 46. Copyright 2023 American Chemical Society.

oxidative homolytic cleavage of water via PCET.[26] Based on these findings, Ehrmaier et al. developed a model[18] wherein they proposed the following reaction mechanism: (1) initial hydrogen bonding from the hydroxylic substrate to the heptazine's nitrogen edge site; (2) photoexcitation followed by PCET from the substrate to form a heptazinyl radical and hydroxyl radical; (3) the cycle is closed by two heptazinyl radicals undergoing thermal radical−radical recombination of two H$^{\bullet}$'s to form H_2. This occurs as the dissociation energy of H_2 is 4.48 eV, so the recombination of two HzH$^{\bullet}$ radicals with dissociation energies of 2.0 eV is an exothermic process.

Recently, Pios and Domcke have focused more specifically on the nature of this intermediate heptazinyl radical species.[27] Carbon nitride has demonstrated a capacity to reduce CO_2[28] to formic acid[29] and methanol.[30] This reaction had been previously modeled as a joint process of water oxidation and carbon dioxide activation via a carbamate complex;[31] however, both proposed steps involve high potential barriers. Pios and Domcke instead proposed that the initial step was an excited state PCET with water to form the heptazinyl radical; this species can then hydrogen bond with CO_2. Subsequent photoexcitation of the intermolecular HzH$^{\bullet}$−CO_2 complex along a repulsive $\pi\sigma^*$ state can drive a barrierless transition to the hydroxyformyl (HOCO) radical.

For both the proposed water oxidation and carbon dioxide reduction mechanisms, the $\pi\sigma^*$ nature of the heptazinyl radical is critical. The heptazinyl radical's planar π-conjugated system mixes with the diffuse antibonding σ^* orbital on the transferred hydrogen,[32] analogous to planar heteroaromatics such as phenol,[33,34] indole,[35,36] and pyrrole.[37,38] This $\pi\sigma^*$ potential energy surface is repulsive along the N−H stretching coordinate due to the transformation of the 3s Rydberg-type orbital of the NH group toward the 1s valence orbital of the H atom upon stretching of the N−H bond. These dark $\pi\sigma^*$ states are often characterized by gas-phase photodissociation experiments.[39,40] Since we are dealing with an intermediate in an excited state PCET reaction, here we adapt ultrafast pump−push−probe spectroscopy,[41−43] in what we term "pump−photolysis−probe" spectroscopy (Figure S1), to experimentally demonstrate for the first time the photodissociation of H$^{\bullet}$ from a transient radical through a $\pi\sigma^*$ state in the condensed phase as displayed in Figure 1.

In the cycle in Figure 1, we are using trianisole heptazine (TAHz, 50 μM) in toluene as the heptazine monomer and methoxyphenol (MeOPhOH, 1M) as the protic substrate. In previous studies on TAHz as a testbed analogue for carbon nitride, we have obtained multiple substantive insights involving kinetic isotope effects,[26] modulating the position of the charge transfer state toward PCET,[44] and how hydrogen bonding affects the vibrational dynamics leading to PCET.[45] These studies were all related to the detailed kinetics of the first three steps of compounds **1a**−**1c** in Figure 1. We have also previously studied the PCET step (Figure 2a) of this system using pump−push−probe spectroscopy.[41] In our prior work, TAHz was incubated with a series of phenolic substrates, to which it can hydrogen bond, ranging from weakly electron withdrawing species, such as phenol, to the most electron donating like 4-methoxyphenol. This range of electron donating and withdrawing character provides the ability to tune the height of the barrier to the charge transfer (CT) state. Initial pump pulses were used to excite the TAHz:R-PhOH complex **1b** to higher S_n $\pi\pi^*$ states, and as it relaxes from higher S_n states to the S_1 state, a fraction branches into the CT state dependent on the height of that barrier.[44] A push pulse of

https://doi.org/10.1021/acsphyschemau.4c00030
ACS Phys. Chem Au 2024, 4, 598−604

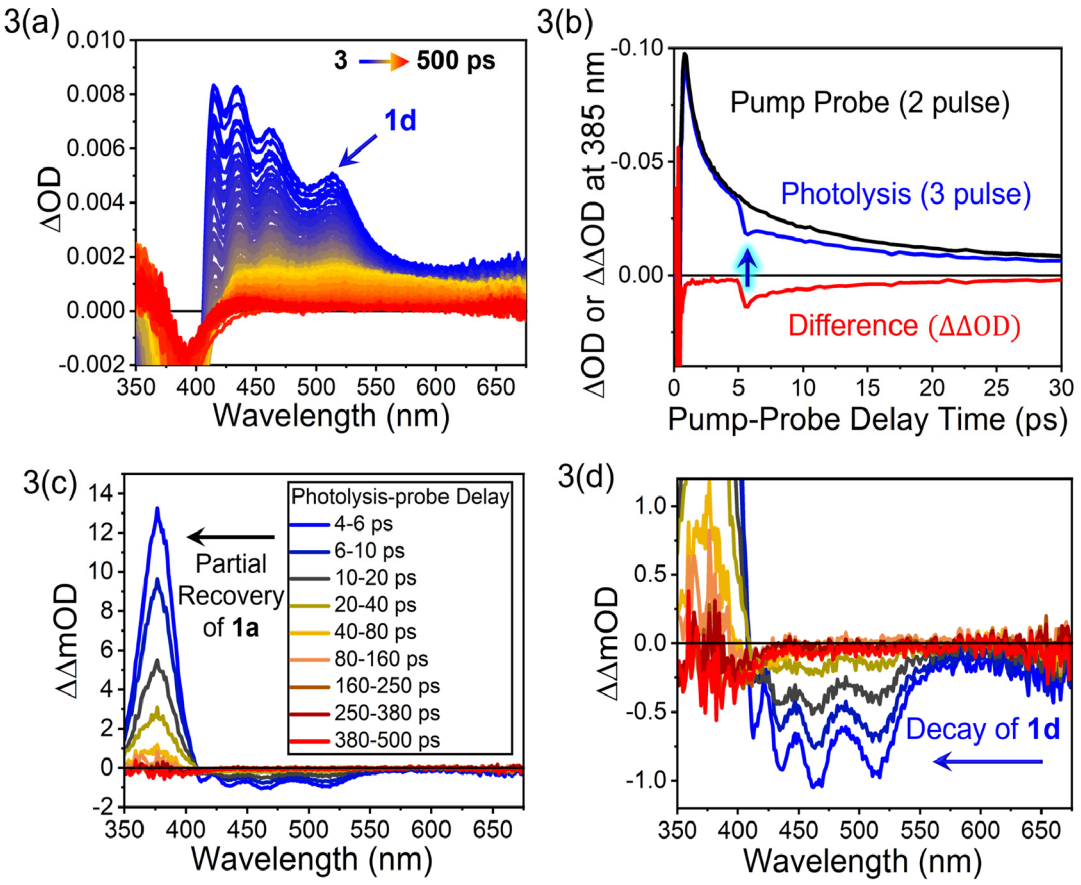

Figure 3. Transient absorption pump−probe and pump−photolysis−probe data of heptazine. (a) Pump−probe spectrum (375 nm excitation) of the TAHz:MeOPhOH complex showing ground state bleach and 520 nm photoproduct absorption signature of the TAHzH$^{\bullet}$ radical generated by PCET. (b) Kinetic trace of TAHz-MeOPhOH ground state bleach (GSB) at 385 nm. Upon the arrival of the third photolysis pulse (375 nm) at $t_{pump-probe}$ = 6 ps, there is a partial ground state recovery, corresponding to the conversion of **1d** to **1a**. (c) Pump−photolysis−probe spectrum highlighting the recovery of the ground state bleach **1a** upon arrival of the photolysis pulse, indicating partial recovery of ground state TAHz as per Figure 1. (d) Magnified view of ΔΔOD spectrum from Figure 3c revealing photodissociation of the TAHzH$^{\bullet}$ radical generated by the pump, which is kinetically linked to the recovery of the ground state bleach, indicating direct conversion between these two states, and releasing H$^{\bullet}$.

Table 1. Doublet Vertical Excitation Energies of TAHzH$^{\bullet}$ Open Shell Radical Species Calculated by ADC(2)

state	energy (eV)	f	dipole moment (D)
$D_1A'(\pi\pi^*)$	1.00	0.013	9.93
$D_2A'(\pi\pi^*)$	1.13	0.067	5.16
$D_3A''(\pi\sigma^*)$	2.88	0.001	11.2
$D_4A'(\pi\pi^*)$	3.03	0.050	4.87
$D_5A'(\pi\pi^*)$	3.24	0.128	5.32
$D_6A'(\pi\pi^*)$	3.32	0.060	3.45

1150 nm (∼1.07 eV) was chosen to allow for a re-excitation of the remaining excited state population in the S_1 state at **1c** back into the CT state. We observed that the decay kinetics of the S_1 state of **1c** correlated with the predicted CT state barrier height, and in the case of 4-methoxyphenol it proved to be a barrierless transition. The main limitation of this previous study was that we were without a clear photoproduct signal, leaving us to monitor the kinetics using depletion of the excited state population of **1c**.

Recently, we published a study[46] where we were able to identify a spectroscopic signature for the photogenerated TAHzH$^{\bullet}$ radical **1d** in the transient absorption (TA) spectrum by varying the local hydrogen bonding environment. In the case of a hydrogen bond accepting solvent such as pyridine[47] where preassociation before PCET cannot occur, the TAHz **1a** TA spectrum is regenerated as per Figure 2d. In the case of toluene, we identified the TAHzH$^{\bullet}$ radical **1d** at ∼520 nm, shown in Figure 2e.

While our prior work uncovered the spectral fingerprint of the TAHzH$^{\bullet}$ radical **1d**, it did little to reveal the fate of this photoproduct and whether it would undergo the predicted photodissociation that would be indicative of having a $\pi\sigma^*$ dissociative state. To explore this photodissociation process, we first performed a pump−probe experiment to reconfirm the presence of the 520 nm signal shown in Figure 3a. We selected a pump pulse wavelength at 375 nm to specifically target the hydrogen bonded TAHz:MeOPhOH **1b** complex that can be seen in the red-shifted absorption of Figure 2c, proceeding the reaction in Figure 2a, and producing the 520 nm TAHzH$^{\bullet}$ radical signature. In addition, we performed a pump power dependence of this signal (Figure S2) revealing a linear power dependence of this signal corresponding to the first order growth of the spectral peak of the TAHzH$^{\bullet}$ radical (**1d**) in response to pump power.

We then introduced a photolysis pulse, also at 375 nm, that would arrive 6 ps after the pump pulse and observed a partial recovery of the ground state bleach in the TAHz-MeOPhOH kinetic trace at 385 nm as seen in Figure 3b. This is the

https://doi.org/10.1021/acsphyschemau.4c00030
ACS Phys. Chem Au 2024, 4, 598−604

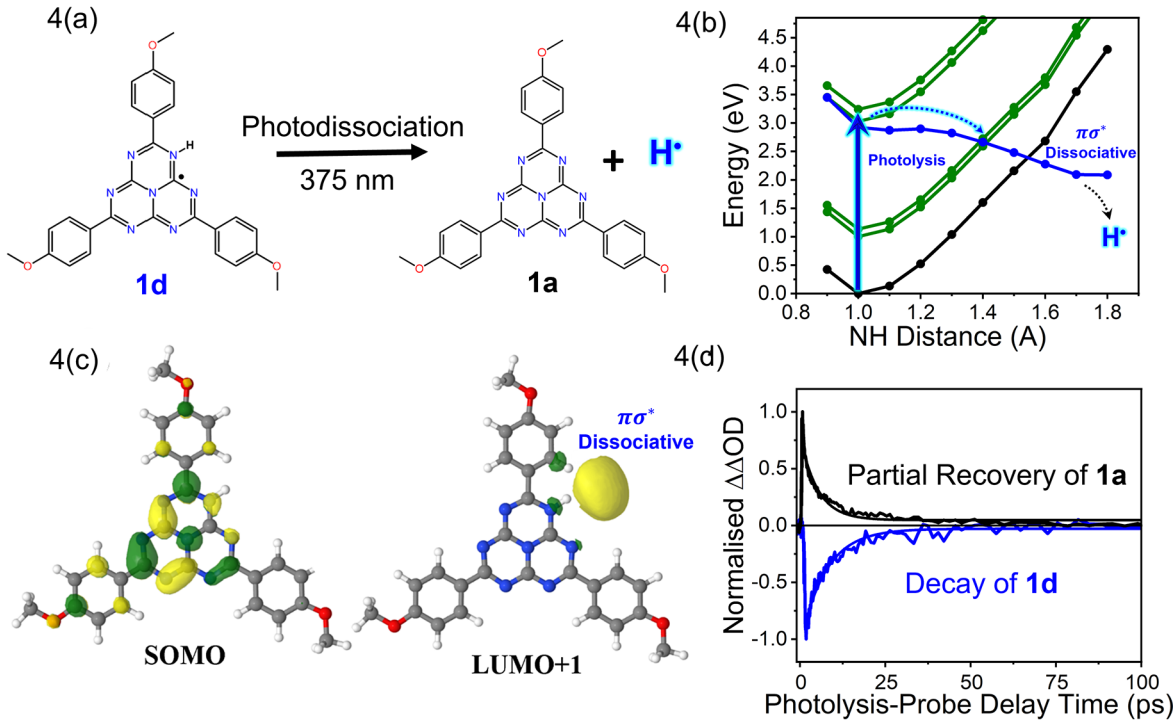

Figure 4. Photolysis reaction step. (a) Photolysis pulse at 375 nm results in photodissociation of the intermediate TAHzH• heptazinyl radical in **1d** to produce closed shell ground state TAHz **1a**. This releases H• in direct response. (b) Rigid scan of TAHzH• energy levels seen in Table 1 along the NH distance at the ADC(2) level (unannotated in Figure S5). Excitation into higher lying $\pi\pi^*$ states with higher oscillator strength, from where it can vibrationally relax along the D_3 $\pi\sigma^*$ state dissociating to regenerate the ground state and releasing H•. Black, electronic ground state; green, $\pi\pi^*$ excited states; blue, $\pi\sigma^*$ excited state. (c) SOMO and LUMO+1 molecular orbitals showing diffuse $\pi\sigma^*$ molecular orbital. (d) Kinetic evolution of **1a** and **1d** signals in response to arrival of the third photolysis pulse at $t_{pump-probe}$ = 6 ps, the arrival of the photolysis pulse reset to time zero. In black, recovery of the ground state bleach is seen in Figure 3c, which is the repopulation of **1a** with a lifetime of τ = 6.6 ± 0.3 ps. In blue is seen the decay of the TAHzH• photoproduct absorption seen in Figure 3d, which is the depopulation of **1d** with a lifetime of τ = 7.0 ± 0.4 ps.

opposite behavior seen in a TAHz only case where a third pulse repumps and increases the GSB (Figure S3). While in our prior work we targeted **1c** with a low energy push pulse at 1150 nm (~1.07 eV) to investigate the barrier of the PCET step, this time we were guided by second-order algebraic-diagrammatic construction scheme (ADC(2)) calculations (Table 1) to target the intermediate TAHzH• radical species **1d** with a higher energy photolysis pulse such as 375 nm (~3.3 eV). By monitoring, in response to the photolysis pulse, the relative populations of **1d** and **1a**, we can directly observe the photolysis reaction and release of H•.

The pump−photolysis−probe spectrum ΔΔOD seen in Figure 3c and magnified in Figure 3d is generated by subtracting the pump−probe spectrum from the pump−photolysis−probe spectrum to isolate the spectral changes caused by the photolysis pulse (ΔOD data can be seen in Figure S4). The positive peak at wavelengths near 370−380 nm in the ΔΔOD spectrum is attributable to a recovery of **1a**, causing a partial ground state recovery (i.e., decreasing the amplitude of the ground state bleach signal) of **1a** seen in the ΔOD spectrum. On the same time scale, a new negative ΔΔOD signal emerges in the 520 nm region. This negative signal in the ΔΔOD is the loss of the **1d** photoproduct absorption signal seen in the ΔOD spectrum. This provides the key piece of experimental evidence. We know that the 520 nm signal is the TAHzH• radical signature, and we know that we can target its $\pi\sigma^*$ dissociative state. If in response to the photolysis pulse, the 520 nm **1d** signal is lost on the same time scale as **1a** is regenerated, just as the mechanism in Figure 1 suggests, it can be kinetically deduced that photodissociation occurs. This necessitates the corresponding release of H• species and demonstrates the $\pi\sigma^*$ nature of the TAHzH• radical dissociation.

The link between the ground state recovery of **1a** and the decay of the TAHzH• radical absorption signature **1d** is particularly clear when the kinetics traces of the averaged 375−380 nm ground state bleach recovery and the averaged 515−520 nm TAHzH• radical absorption decay are plotted together. Both progress on commensurate time scales of 6.6 ± 0.3 and 7.0 ± 0.4 ps as seen in Figure 4d, clearly indicating the photodissociation outlined in the fourth step of Figure 1 and the reaction in Figure 4a.

The TAHzH• radical, like the pyridinyl radical,[48] has a singly occupied molecular orbital (SOMO) with π character, resulting in a minimal probability of direct excitation into the $\pi\sigma^*$ state, necessitating excitation into higher $\pi\pi^*$ states and radiationless transfer through a conical intersection into the $\pi\sigma^*$ state.[32] Table 1 displays the relevant doublet excited states of the TAHzH• radical. The photolysis pulse at 375 nm excites bright $\pi\pi^*$ states D_5 and D_6 with higher oscillator strength, from where it can vibrationally relax along the dark $\pi\sigma^*$ state dissociating to regenerate the ground state and releasing H•.

These results demonstrate that we are able to photochemically cycle TAHzH• and release H•, a compelling prospect if used as a photoreductant.[49,50] The spectroscopic assignments of this work identify the TAHzH• heptazinyl radical and its photodissociation behavior through a $\pi\sigma^*$ state, which is

https://doi.org/10.1021/acsphyschemau.4c00030
ACS Phys. Chem Au 2024, 4, 598−604

experimental evidence for proposed mechanisms of heptazine and carbon nitride photoreactivity involving radical intermediates for PCET.[17,27] New heptazine derivatives with increased solubility could enhance our understanding of heptazine photoreactivity. Due to the insolubility of current heptazines in suitable solvents for time-resolved infrared spectroscopy (TRIR),[51,52] we have recently synthesized a new highly soluble heptazine using Friedel−Crafts between trichloroheptazine and [(2-ethylhexyl)oxy]benzene. This may allow us to directly probe the importance of vibronic coupling for this $\pi\sigma^*$ dependent photoreaction.[53] To test the predicted barrierless excited state PCET between the heptazinyl radical and CO_2,[27] one could synthesize a water-soluble heptazine monomer, which could then form heptazinyl radicals from water by PCET and, with a subsequent UV pulse, reduce CO_2.

■ ASSOCIATED CONTENT

Supporting Information

The Supporting Information is available free of charge at https://pubs.acs.org/doi/10.1021/acsphyschemau.4c00030.

Details of TAHz synthesis, transient absorption setup, pump−probe and pump−photolysis−probe measurements, raw data of pump−photolysis−probe measurements, power dependence of TAHz-H at 520 nm from pump pulse, TAHz only pump−repump−probe control, computational methods, details of rigid scan of TAHzH along the NH distance (PDF)

■ AUTHOR INFORMATION

Corresponding Author

Cody W. Schlenker − *Department of Chemistry, University of Washington, Seattle, Washington 98195, United States; Molecular Engineering and Sciences Institute, University of Washington, Seattle, Washington 98195-1652, United States; Clean Energy Institute, University of Washington, Seattle, Washington 98195-1653, United States;* orcid.org/0000-0003-3103-402X; Email: schlenk@uw.edu

Authors

Liam Wrigley − *Department of Chemistry, University of Washington, Seattle, Washington 98195, United States;* orcid.org/0000-0003-3394-5054

Doyk Hwang − *Department of Chemistry, University of Washington, Seattle, Washington 98195, United States*

Sebastian V. Pios − *Zhejiang Laboratory, Hangzhou 311100, China*

Complete contact information is available at: https://pubs.acs.org/10.1021/acsphyschemau.4c00030

Author Contributions

⊥These authors contributed equally to this work. CRediT: **Liam M Wrigley** data curation, formal analysis, investigation, project administration, visualization, writing-original draft, writing-review & editing; **Doyk Hwang** conceptualization, formal analysis, investigation, methodology, supervision, validation, writing-review & editing; **Sebastian V Pios** formal analysis, investigation, software, writing-review & editing; **Cody W. Schlenker** conceptualization, funding acquisition, project administration, resources, supervision, writing-review & editing.

Notes

The authors declare no competing financial interest.

■ ACKNOWLEDGMENTS

We would like to express our deep appreciation to Prof. Dr. Wolfgang Domcke and Prof. Dr. Andrzej Sobolewski for sharing detailed thoughtful insight and feedback during the development of this work. This work is based on research that was supported in part by the Washington Research Foundation and the University of Washington Clean Energy Institute (CEI). Part of this work was conducted at the Molecular Analysis Facility, a National Nanotechnology Coordinated Infrastructure (NNCI) site at the University of Washington, which is supported in part by funds from the National Science Foundation (awards NNCI-2025489, NNCI-542101), the Molecular Engineering and Sciences Institute, and the Clean Energy Institute. C.W.S. acknowledges that a portion of this material is based upon work supported by the U.S. National Science Foundation (NSF) under Grant No. [1846480]. S.V.P. acknowledges support from the starting grant of research center of new materials computing of Zhejiang Lab (No. 3700-32601).

■ REFERENCES

(1) Nocera, D. G. Proton-Coupled Electron Transfer: The Engine of Energy Conversion and Storage. *J. Am. Chem. Soc.* **2022**, *144* (3), 1069−1081.

(2) Tyburski, R.; Liu, T.; Glover, S. D.; Hammarström, L. Proton-Coupled Electron Transfer Guidelines, Fair and Square. *J. Am. Chem. Soc.* **2021**, *143* (2), 560−576.

(3) Mora, S. J.; Odella, E.; Moore, G. F.; Gust, D.; Moore, T. A.; Moore, A. L. Proton-Coupled Electron Transfer in Artificial Photosynthetic Systems. *Acc. Chem. Res.* **2018**, *51* (2), 445−453.

(4) Hammarström, L.; Styring, S. Proton-coupled electron transfer of tyrosines in Photosystem II and model systems for artificial photosynthesis: the role of a redox-active link between catalyst and photosensitizer. *Energy Environ. Sci.* **2011**, *4* (7), 2379−2388.

(5) Saura, P.; Kaila, V. R. I. Energetics and Dynamics of Proton-Coupled Electron Transfer in the NADH/FMN Site of Respiratory Complex I. *J. Am. Chem. Soc.* **2019**, *141* (14), 5710−5719.

(6) Hammes-Schiffer, S.; Stuchebrukhov, A. A. Theory of coupled electron and proton transfer reactions. *Chem. Rev.* **2010**, *110* (12), 6939−6960.

(7) Murray, P. R. D.; Cox, J. H.; Chiappini, N. D.; Roos, C. B.; McLoughlin, E. A.; Hejna, B. G.; Nguyen, S. T.; Ripberger, H. H.; Ganley, J. M.; Tsui, E.; Shin, N. Y.; Koronkiewicz, B.; Qiu, G.; Knowles, R. R. Photochemical and Electrochemical Applications of Proton-Coupled Electron Transfer in Organic Synthesis. *Chem. Rev.* **2022**, *122* (2), 2017−2291.

(8) Domcke, W.; Sobolewski, A. L.; Schlenker, C. W. Photooxidation of water with heptazine-based molecular photocatalysts: Insights from spectroscopy and computational chemistry. *J. Chem. Phys.* **2020**, *153* (10), 100902.

(9) Ong, W.-J.; Tan, L.-L.; Ng, Y. H.; Yong, S.-T.; Chai, S.-P. Graphitic Carbon Nitride (g-C3N4)-Based Photocatalysts for Artificial Photosynthesis and Environmental Remediation: Are We a Step Closer To Achieving Sustainability? *Chem. Rev.* **2016**, *116* (12), 7159−7329.

(10) Rono, N.; Kibet, J. K.; Martincigh, B. S.; Nyamori, V. O. A review of the current status of graphitic carbon nitride. *Crit. Rev. Solid State Mater. Sci.* **2021**, *46* (3), 189−217.

(11) Lau, V. W. -h.; Mesch, M. B.; Duppel, V.; Blum, V.; Senker, J.; Lotsch, B. V. Low-Molecular-Weight Carbon Nitrides for Solar Hydrogen Evolution. *J. Am. Chem. Soc.* **2015**, *137* (3), 1064−1072.

(12) Hwang, D.; Schlenker, C. W. Photochemistry of carbon nitrides and heptazine derivatives. *Chem. Commun.* **2021**, *57* (74), 9330−9353.
(13) Wang, X.; Maeda, K.; Thomas, A.; Takanabe, K.; Xin, G.; Carlsson, J. M.; Domen, K.; Antonietti, M. A metal-free polymeric photocatalyst for hydrogen production from water under visible light. *Nat. Mater.* **2009**, *8* (1), 76−80.
(14) Tang, J.; Durrant, J. R.; Klug, D. R. Mechanism of photocatalytic water splitting in TiO2. Reaction of water with photoholes, importance of charge carrier dynamics, and evidence for four-hole chemistry. *J. Am. Chem. Soc.* **2008**, *130* (42), 13885−13891.
(15) Cowan, A. J.; Durrant, J. R. Long-lived charge separated states in nanostructured semiconductor photoelectrodes for the production of solar fuels. *Chem. Soc. Rev.* **2013**, *42* (6), 2281−2293.
(16) Takanabe, K. Photocatalytic water splitting: quantitative approaches toward photocatalyst by design. *ACS Catal.* **2017**, *7* (11), 8006−8022.
(17) Ehrmaier, J.; Karsili, T. N. V.; Sobolewski, A. L.; Domcke, W. Mechanism of Photocatalytic Water Splitting with Graphitic Carbon Nitride: Photochemistry of the Heptazine−Water Complex. *J. Phys. Chem. A* **2017**, *121* (25), 4754−4764.
(18) Ehrmaier, J.; Domcke, W.; Opalka, D. Mechanism of Photocatalytic Water Oxidation by Graphitic Carbon Nitride. *J. Phys. Chem. Lett.* **2018**, *9* (16), 4695−4699.
(19) Ullah, N.; Chen, S.; Zhao, Y.; Zhang, R. Photoinduced Water-Heptazine Electron-Driven Proton Transfer: Perspective for Water Splitting with g-C(3)N(4). *J. Phys. Chem. Lett.* **2019**, *10* (15), 4310−4316.
(20) You, P.; Lian, C.; Chen, D.; Xu, J.; Zhang, C.; Meng, S.; Wang, E. Nonadiabatic Dynamics of Photocatalytic Water Splitting on A Polymeric Semiconductor. *Nano Lett.* **2021**, *21* (15), 6449−6455.
(21) Savateev, O.; Nolkemper, K.; Kühne, T. D.; Shvalagin, V.; Markushyna, Y.; Antonietti, M. Extent of carbon nitride photocharging controls energetics of hydrogen transfer in photochemical cascade processes. *Nat. Commun.* **2023**, *14* (1), 7684.
(22) Markushyna, Y.; Smith, C. A.; Savateev, A. Organic Photocatalysis: Carbon Nitride Semiconductors vs. *Molecular Catalysts. Eur. J. Org. Chem.* **2020**, *2020* (10), 1294−1309.
(23) Merschjann, C.; Tyborski, T.; Orthmann, S.; Yang, F.; Schwarzburg, K.; Lublow, M.; Lux-Steiner, M.-C.; Schedel-Niedrig, T. Photophysics of polymeric carbon nitride: An optical quasimonomer. *Phys. Rev. B* **2013**, *87* (20), 205204.
(24) Kuzkova, N.; Kiyan, I. Y.; Wilkinson, I.; Merschjann, C. Ultrafast dynamics in polymeric carbon nitride thin films probed by time-resolved EUV photoemission and UV-Vis transient absorption spectroscopy. *Phys. Chem. Chem. Phys.* **2023**, *25* (40), 27094−27113.
(25) Godin, R.; Wang, Y.; Zwijnenburg, M. A.; Tang, J.; Durrant, J. R. Time-Resolved Spectroscopic Investigation of Charge Trapping in Carbon Nitrides Photocatalysts for Hydrogen Generation. *J. Am. Chem. Soc.* **2017**, *139* (14), 5216−5224.
(26) Rabe, E. J.; Corp, K. L.; Sobolewski, A. L.; Domcke, W.; Schlenker, C. W. Proton-Coupled Electron Transfer from Water to a Model Heptazine-Based Molecular Photocatalyst. *J. Phys. Chem. Lett.* **2018**, *9* (21), 6257−6261.
(27) Pios, S.; Domcke, W. Ab Initio Electronic Structure Study of the Photoinduced Reduction of Carbon Dioxide with the Heptazinyl Radical. *J. Phys. Chem. A* **2022**, *126* (18), 2778−2787.
(28) He, M.; Fang, Z.; Wang, P.; You, Y.; Li, Z. Recent progress in photocatalytic chemical fixation of carbon dioxide. *ACS Sustainable Chem. Eng.* **2023**, *11* (33), 12194−12217.
(29) Pachaiappan, R.; Rajendran, S.; Senthil Kumar, P.; Vo, D.-V. N.; Hoang, T. K. A. A review of recent progress on photocatalytic carbon dioxide reduction into sustainable energy products using carbon nitride. *Chem. Eng. Res. Des.* **2022**, *177*, 304−320.
(30) Khan, J.; Sun, Y.; Han, L. A Comprehensive Review on Graphitic Carbon Nitride for Carbon Dioxide Photoreduction. *Small Methods* **2022**, *6* (12), 2201013.
(31) Wu, H.-Z.; Bandaru, S.; Huang, X.-L.; Liu, J.; Li, L.-L.; Wang, Z. Theoretical insight into the mechanism of photoreduction of CO 2 to CO by graphitic carbon nitride. *Phys. Chem. Chem. Phys.* **2019**, *21* (3), 1514−1520.
(32) Sobolewski, A. L.; Domcke, W.; Dedonder-Lardeux, C.; Jouvet, C. Excited-state hydrogen detachment and hydrogen transfer driven by repulsive 1 $\pi\sigma^*$ states: A new paradigm for nonradiative decay in aromatic biomolecules. *Phys. Chem. Chem. Phys.* **2002**, *4* (7), 1093−1100.
(33) Sobolewski, A. L.; Domcke, W. Photoinduced Electron and Proton Transfer in Phenol and Its Clusters with Water and Ammonia. *J. Phys. Chem. A* **2001**, *105* (40), 9275−9283.
(34) Lan, Z.; Domcke, W.; Vallet, V.; Sobolewski, A. L.; Mahapatra, S. Time-dependent quantum wave-packet description of the $\pi1\sigma^*$ photochemistry of phenol. *J. Chem. Phys.* **2005**, *122* (22), 224315.
(35) Sobolewski, A. L.; Domcke, W. Ab initio investigations on the photophysics of indole. *Chem. Phys. Lett.* **1999**, *315* (3), 293−298.
(36) Sobolewski, A. L.; Domcke, W. Photoinduced charge separation in indole−water clusters. *Chem. Phys. Lett.* **2000**, *329* (1), 130−137.
(37) Vallet, V.; Lan, Z.; Mahapatra, S.; Sobolewski, A. L.; Domcke, W. Time-dependent quantum wave-packet description of the $1\pi\sigma^*$ photochemistry of pyrrole. *Faraday Discuss.* **2004**, *127* (0), 283−293.
(38) Vallet, V.; Lan, Z.; Mahapatra, S.; Sobolewski, A. L.; Domcke, W. Photochemistry of pyrrole: time-dependent quantum wave-packet description of the dynamics at the 1pi sigma*-S0 conical intersections. *J. Chem. Phys.* **2005**, *123* (14), 144307.
(39) Ashfold, M. N. R.; King, G. A.; Murdock, D.; Nix, M. G. D.; Oliver, T. A. A.; Sage, A. G. $\pi\sigma^*$ excited states in molecular photochemistry. *Phys. Chem. Chem. Phys.* **2010**, *12* (6), 1218−1238.
(40) Ashfold, M. N. R.; Murdock, D.; Oliver, T. A. A. Molecular Photofragmentation Dynamics in the Gas and Condensed Phases. *Annu. Rev. Phys. Chem.* **2017**, *68* (1), 63−82.
(41) Corp, K. L.; Rabe, E. J.; Huang, X.; Ehrmaier, J.; Kaiser, M. E.; Sobolewski, A. L.; Domcke, W.; Schlenker, C. W. Control of Excited-State Proton-Coupled Electron Transfer by Ultrafast Pump-Push-Probe Spectroscopy in Heptazine-Phenol Complexes: Implications for Photochemical Water Oxidation. *J. Phys. Chem. C* **2020**, *124* (17), 9151−9160.
(42) Bakulin, A. A.; Rao, A.; Pavelyev, V. G.; van Loosdrecht, P. H. M.; Pshenichnikov, M. S.; Niedzialek, D.; Cornil, J.; Beljonne, D.; Friend, R. H. The Role of Driving Energy and Delocalized States for Charge Separation in Organic Semiconductors. *Science* **2012**, *335* (6074), 1340−1344.
(43) Paternò, G. M.; Moretti, L.; Barker, A. J.; Chen, Q.; Müllen, K.; Narita, A.; Cerullo, G.; Scotognella, F.; Lanzani, G. Pump−Push−Probe for Ultrafast All-Optical Switching: The Case of a Nanographene Molecule. *Adv. Funct. Mater.* **2019**, *29* (21), 1805249.
(44) Rabe, E. J.; Corp, K. L.; Huang, X.; Ehrmaier, J.; Flores, R. G.; Estes, S. L.; Sobolewski, A. L.; Domcke, W.; Schlenker, C. W. Barrierless Heptazine-Driven Excited State Proton-Coupled Electron Transfer: Implications for Controlling Photochemistry of Carbon Nitrides and Aza-Arenes. *J. Phys. Chem. C* **2019**, *123* (49), 29580−29588.
(45) Rabe, E. J.; Goldwyn, H. J.; Hwang, D.; Masiello, D. J.; Schlenker, C. W. Intermolecular Hydrogen Bonding Tunes Vibronic Coupling in Heptazine Complexes. *J. Phys. Chem. B* **2020**, *124* (51), 11680−11689.
(46) Hwang, D.; Wrigley, L. M.; Lee, M.; Sobolewski, A. L.; Domcke, W.; Schlenker, C. W. Local Hydrogen Bonding Determines Branching Pathways in Intermolecular Heptazine Photochemistry. *J. Phys. Chem. B* **2023**, *127* (30), 6703−6713.
(47) Laurence, C.; Brameld, K. A.; Graton, J.; Le Questel, J. Y.; Renault, E. The pK(BHX) database: toward a better understanding of hydrogen-bond basicity for medicinal chemists. *J. Med. Chem.* **2009**, *52* (14), 4073−86.
(48) Ehrmaier, J.; Picconi, D.; Karsili, T. N. V.; Domcke, W. Photodissociation dynamics of the pyridinyl radical: Time-dependent quantum wave-packet calculations. *J. Chem. Phys.* **2017**, *146* (12), 124304.

https://doi.org/10.1021/acsphyschemau.4c00030
ACS Phys. Chem Au 2024, 4, 598−604

(49) Le Saux, E.; Georgiou, E.; Dmitriev, I. A.; Hartley, W. C.; Melchiorre, P. Photochemical Organocatalytic Functionalization of Pyridines via Pyridinyl Radicals. *J. Am. Chem. Soc.* **2023**, *145* (1), 47−52.
(50) MacKenzie, I. A.; Wang, L.; Onuska, N. P. R.; Williams, O. F.; Begam, K.; Moran, A. M.; Dunietz, B. D.; Nicewicz, D. A. Discovery and characterization of an acridine radical photoreductant. *Nature* **2020**, *580* (7801), 76−80.
(51) Mezzetti, A.; Schnee, J.; Lapini, A.; Di Donato, M. Time-resolved infrared absorption spectroscopy applied to photoinduced reactions: how and why. *Photochem. Photobiol. Sci.* **2022**, *21* (4), 557−584.
(52) Hare, P. M.; Middleton, C. T.; Mertel, K. I.; Herbert, J. M.; Kohler, B. Time-resolved infrared spectroscopy of the lowest triplet state of thymine and thymidine. *Chem. Phys.* **2008**, *347* (1), 383−392.
(53) Murdock, D.; Harris, S. J.; Karsili, T. N. V.; Greetham, G. M.; Clark, I. P.; Towrie, M.; Orr-Ewing, A. J.; Ashfold, M. N. R. Photofragmentation Dynamics in Solution Probed by Transient IR Absorption Spectroscopy: $\pi\sigma^*$-Mediated Bond Cleavage in p-Methylthiophenol and p-Methylthioanisole. *J. Phys. Chem. Lett.* **2012**, *3* (24), 3715−3720.

https://doi.org/10.1021/acsphyschemau.4c00030
ACS Phys. Chem Au 2024, 4, 598−604